Available online at www.sciencedirect.com
SCIENCE DIRECT®

Journal of the European Ceramic Society 24 (2004) 511–516

www.elsevier.com/locate/jeurceramsoc

Effects of rare earth dopants on grain boundary bonding in alumina–silicon carbide composites

Zhen-Yan Deng[a,*], You Zhou[b], Manuel E. Brito[b], Yoshihisa Tanaka[a], Tatsuki Ohji[b]

[a]*Metal Matrix Composite Research Group, National Institute for Materials Science, 1-2-1 Sengen, Tsukuba, Ibaraki 305-0047, Japan*
[b]*Synergy Materials Research Center, National Institute of Advanced Industrial Science and Technology, Nagoya 463-8687, Japan*

Abstract

Effects of trace rare earth impurities on grain boundary bonding in Al_2O_3–5 vol.% SiC composites were investigated. It was found that doping of 800 ppm different rare-earth impurities (Y^{3+}, Nd^{3+} and La^{3+}) led to a fracture-mode change from transgranular in dopant-free composites to intergranular in rare-earth doped composites. The fracture toughness of rare-earth doped composites was higher than that of the composites without dopants, due to an increased crack deflection in doped composites caused by the intergranular fracture. Boundary chemistry analyses showed that rare-earth impurities and Si^{4+} ions both segregated at the Al_2O_3 grain boundaries and resulted in a weak grain boundary bonding.

Keywords: Al_2O_3; Composites; Grain boundary bonding; Rare earth dopants; SiC particles; Al_2O_3/SiC

1. Introduction

It has been shown that trace impurities and additives influence the grain growth and properties of technical ceramics such as high-purity Al_2O_3.[1–3] For example, the addition of MgO causes Al_2O_3 grain-boundary roughening and inhibits abnormal grain growth.[1,3] Codoping of SiO_2 and MgO in Al_2O_3 increases their mutual bulk solid solubility and decreases interfacial segregation over single doping, which is beneficial to improving corrosion resistance of Al_2O_3 ceramics to aqueous HF.[2]

Recently, the effects of doping and codoping of Zr^{4+} and rare-earth impurities in high-purity Al_2O_3 have received considerable attention, due to a significant improvement in high-temperature creep resistance by doping.[4–7] Cho et al.[4] and Yoshida et al.[6] found that doping of 450–1000 ppm Y^{3+}, La^{3+} and Lu^{3+} in Al_2O_3 reduced the creep rate approximately in two orders of magnitude. Wakai et al.[5] found that doping as little as 100 ppm of Zr^{4+} in Al_2O_3 caused the creep hardening effect. Increasing the amount of zirconium dopant further reduced the creep rate. Li et al.[7] found that codoping with ions of differing size can result in an improved creep behavior compared with the singly doped compositions. Further investigations showed that outsize ions segregating to more energetically favorable grain boundary sites, which block a few critical diffusion pathways, are the controlling mechanisms for the improvement in creep resistance of Al_2O_3.[8–12] At the same time, the Al_2O_3 grain boundary was strengthened by doping Zr^{4+} or rare-earth dopants in Al_2O_3.[13]

Al_2O_3–SiC particle composites have been studied for many years,[14–16] since the pioneer work of Niihara.[14] However, the investigations about the effect of trace impurities and additives on the microstructure and mechanical properties of Al_2O_3–SiC composites are not as many as pure Al_2O_3 ceramics. Deng et al.[17,18] found that SiC particles with a thick SiO_2 surface layer were easy to be entrapped in the Al_2O_3 matrix grains such that the oxidation and creep resistance of Al_2O_3–SiC composites was improved considerably. Jeong et al.[19] found that MgO, as a sintering additive, had a key role in improving the densification and controlling the microstructure of Al_2O_3–SiC nanocomposites. In this paper, the effects of rare-earth dopants on the fracture mode and fracture toughness of Al_2O_3–SiC composites are presented.

* Corresponding author. Tel.: +81-298-59-2238; fax: +81-298-59-2201.
E-mail address: deng.zhenyan@nims.go.jp (Z.-Y. Deng).

0955-2219/03/$ - see front matter © 2003 Elsevier Ltd. All rights reserved.
doi:10.1016/S0955-2219(03)00198-5

2. Experimental procedure

The α-Al_2O_3 powder that was used in this study (TM-DAR, 0.21 μm, surface area 13.6 m^2/g, Taimei Chemical Co., Nagano, Japan) had a purity of 99.99%. The α-SiC powder (2.3 μm, Showa Denko Co., Japan) had a purity of 99.7% (F.C: 0.19 wt.%; F.SiO_2: 0.13 wt.%; Fe: 0.008 wt.%; Al: 0.002 wt.%). In order to remove the native SiO_2 on SiC particle surfaces, SiC powder was mixed with a HF aqueous solution for 4–6 hours, then repeatedly washed by a distilled water till a pH value of ~7. A slurry of 5 vol.% SiC + 95 vol.% Al_2O_3 was prepared by using the distilled water. A doping level of 800 ppm (rare-earth ion/Al^{3+} ratio) was achieved by adding an appropriate amount of rare-earth nitrate aqueous solution to the composite slurry. Three types of rare-earth nitrates ($Y(NO_3)_3{\cdot}6H_2O$, purity 99.9%; $Nd(NO_3)_3{\cdot}6H_2O$, purity 99.9%; $La(NO_3)_3{\cdot}6H_2O$, purity 99%; Katayama Chemical Co., Japan) were used in this study. The slurry was milled for 48 h by nylon balls, then dried and sieved using a 100-mesh nylon sieve. To minimize powder contamination, all powder processing was conducted using precleaned Teflon ware under clean-room conditions.

The specimens were fabricated by hot-pressing in a graphite die under an Ar atmosphere for 1 h at 40 MPa. The heating and cooling rates were 15 and 10 °C/min, respectively. The hot-pressing temperature was 1550 °C for all the composites. After they were hot-pressed, all the materials were >99.5% of theoretical density, as measured by the Archimedes method with distilled water as the immersion medium. The hot-pressed specimens were cut into pieces measuring 3 mm×4 mm×25 mm, then ground before toughness measurement. Fracture toughness was measured using the single-edge-precracked-beam (SEPB) method, according to JIS R1607. A span of 16 mm of the three-point bend test and a crosshead speed of 0.5 mm/min were used for strength measurement of the toughness specimens. At least six specimens were used for each toughness point.

A piece of each composite was polished to a 1 μm diamond finish, then indented under a load of 98 N and a dwelling time of 15 s, to observe the crack propagation. The fracture morphology by bending tests and the crack from the corner of indentation were observed by scanning electron microscopy (SEM). The grain morphology and boundary chemistry were analyzed via

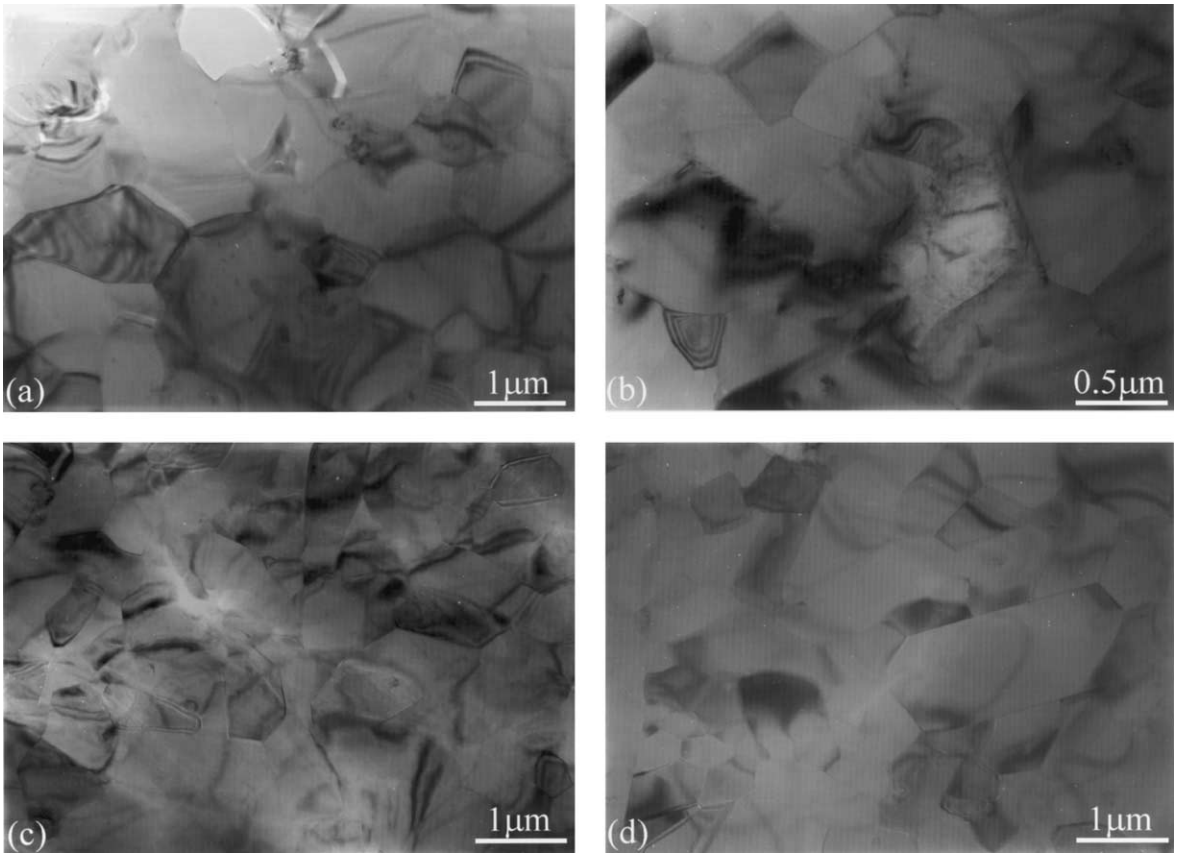

Fig. 1. TEM micrographs of Al_2O_3–SiC composites without dopants (a) and doped with 800 ppm Y^{3+} (b), Nd^{3+} (c) and La^{3+} (d) rare-earth impurities.

transmission electron microscopy (TEM) and high-resolution transmission electron microscopy (HRTEM).

3. Results and discussion

3.1. Grain morphology

Fig. 1 shows the grain morphologies of the Al_2O_3–SiC composites with and without rare-earth dopants. In general, the matrix Al_2O_3 grain sizes of the composites are in the range of 1–2 μm, depending on the type of the dopants. The average Al_2O_3 grain sizes of the composites with rare-earth dopants are smaller than that of the composite without dopants, due to the inhibition effect of rare-earth dopants on Al_2O_3 grain growth[20] (note that the value of scale bar in Fig. 1b is half of those in other three). SiC particles are usually located at the Al_2O_3 grain boundaries. The Al_2O_3 grain morphologies are equiaxed in the composites without dopants and doped with Y^{3+} dopants. However, there are some lathlike Al_2O_3 grains in the Nd^{3+} and La^{3+} doped composites, indicating that these rare-earth dopants caused anisotropic Al_2O_3 grain growth; similar phenomena have been observed in Nd^{3+} and La^{3+} doped pure Al_2O_3 ceramics.[7,21]

3.2. Fracture-mode change

Fig. 2 shows the fracture morphologies of the composites with and without rare-earth dopants after bending tests (note that the value of scale bar in Fig. 2a is 2.5 times of those in other three). It is obvious that transgranular fracture dominates in pure Al_2O_3–SiC composite, as shown in Fig. 2a. This is consistent with other observations on the fracture mode of the Al_2O_3–SiC systems.[19,22–24] To our knowledge, the fracture-mode of the Al_2O_3–SiC composites has been reported to be always transgranular. However, there is an obvious fracture-mode change in rare-earth doped Al_2O_3–SiC composites, that is, the intergranular fracture dominates in these composites, as shown in Fig. 2b–d. Because of the fracture-mode change, the fracture toughness of the Al_2O_3–SiC composites is improved, as listed in Table 1.

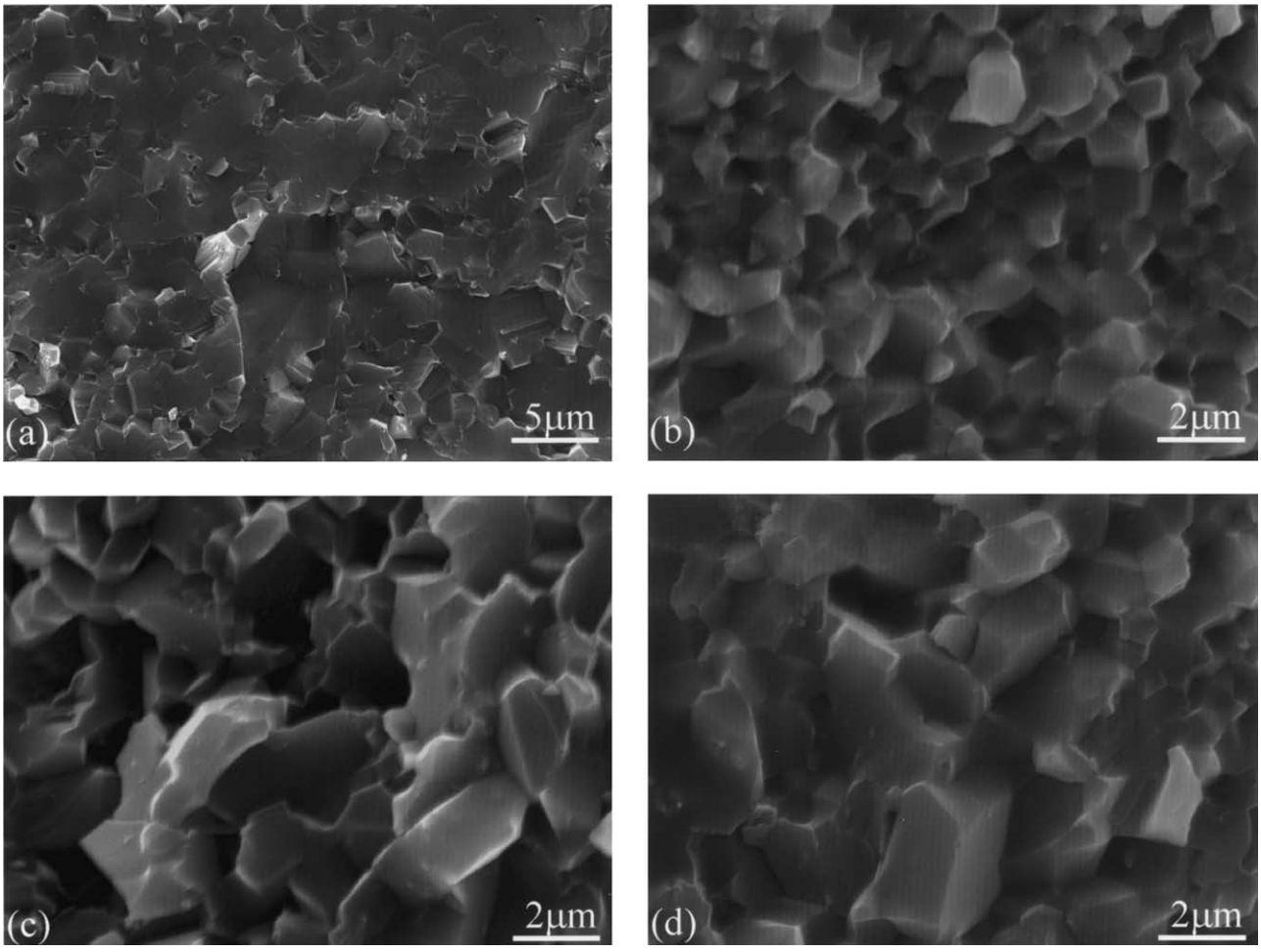

Fig. 2. SEM micrographs of the fracture surfaces of Al_2O_3–SiC composites without dopants (a) and doped with 800 ppm Y^{3+} (b), Nd^{3+} (c) and La^{3+} (d) rare-earth impurities.

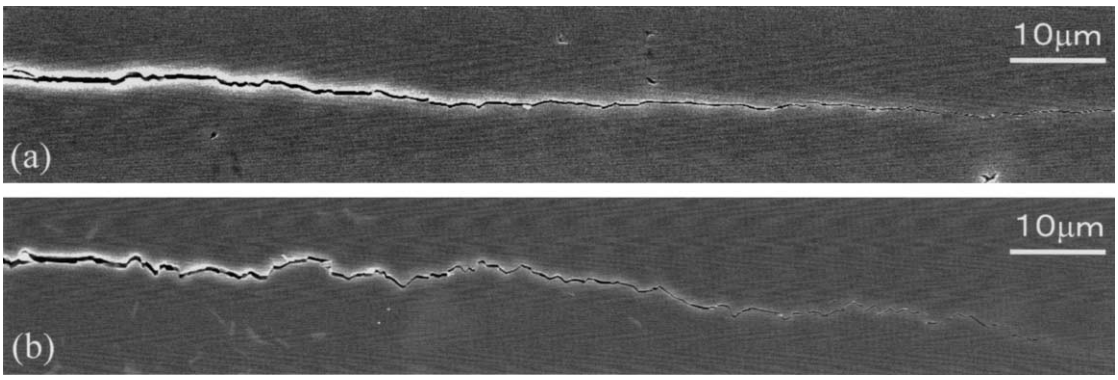

Fig. 3. SEM micrographs of the crack propagation in Al_2O_3–SiC composites without dopants (a) and doped with 800 ppm La^{3+} rare-earth impurities (b).

For example, doping of 800 ppm La^{3+} in Al_2O_3–SiC composite increased the fracture toughness up to ~5.0 MPa·$m^{1/2}$, a value of 1.5 times of the fracture toughness of the dopant-free composite. Moreover, the improvements in fracture toughness by doping with Nd^{3+} and La^{3+} are more obvious than those by doping with Y^{3+}.

Fig. 3 shows the crack propagation in a dopant-free composite and an La^{3+} doped composite. The intergranular fracture in La^{3+}-doped composite significantly increased the crack deflection, compared to the dopant-free composite; similar phenomena were found in other rare-earth doped composites. It is well known that crack deflection increases the critical strain energy release rate.[25] Therefore, the increase in crack deflection in rare-earth doped composites is an important mechanism to increase their toughness. Because the grain size of Y^{3+} doped composite is smaller than that of the dopant-free composite and its grain morphology is equiaxed (Fig. 1), and the fracture toughness of Y^{3+} doped composite was improved slightly relative to that of the dopant-free composite. As some lathlike Al_2O_3 grains existed in Nd^{3+} and La^{3+} doped composites, pullout and bridging occurred during crack propagation, like whiskers; these result in the higher fracture toughness of Nd^{3+} and La^{3+} doped composites than that of Y^{3+} doped composite. In fact, some pits left behind by the pullouts of the lathlike Al_2O_3 gains can be clearly seen in the fracture surfaces of Nd^{3+} and La^{3+} doped composites, as shown in Fig. 2c and d.

Table 1
Fracture toughness of Al_2O_3–5 vol.% SiC composites with different rare-earth dopants

Dopant	Fracture toughness (MPa·$m^{1/2}$)
Pure	3.34±0.61
800 ppm Y^{3+}	3.66±0.42
800 ppm Nd^{3+}	4.79±0.69
800 ppm La^{3+}	5.04±0.72

Usually, the fracture mode in pure Al_2O_3 ceramics is intergranular.[13,22] The transgranular fracture in conventional Al_2O_3–SiC composites results from a strengthened Al_2O_3 grain boundary due to the existence of SiC particles.[15,24] Therefore, it can be deduced that the fracture mode change in rare-earth doped Al_2O_3–SiC composites is due to a weakened Al_2O_3 grain boundary bonding.

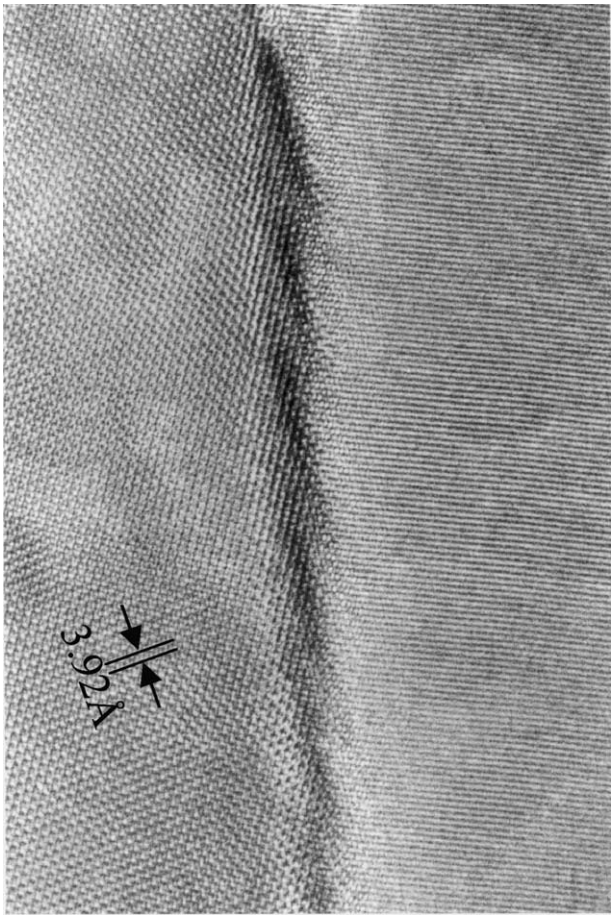

Fig. 4. HRTEM micrograph of a typical grain boundary between two Al_2O_3 grains in Y^{3+} doped Al_2O_3–SiC composite.

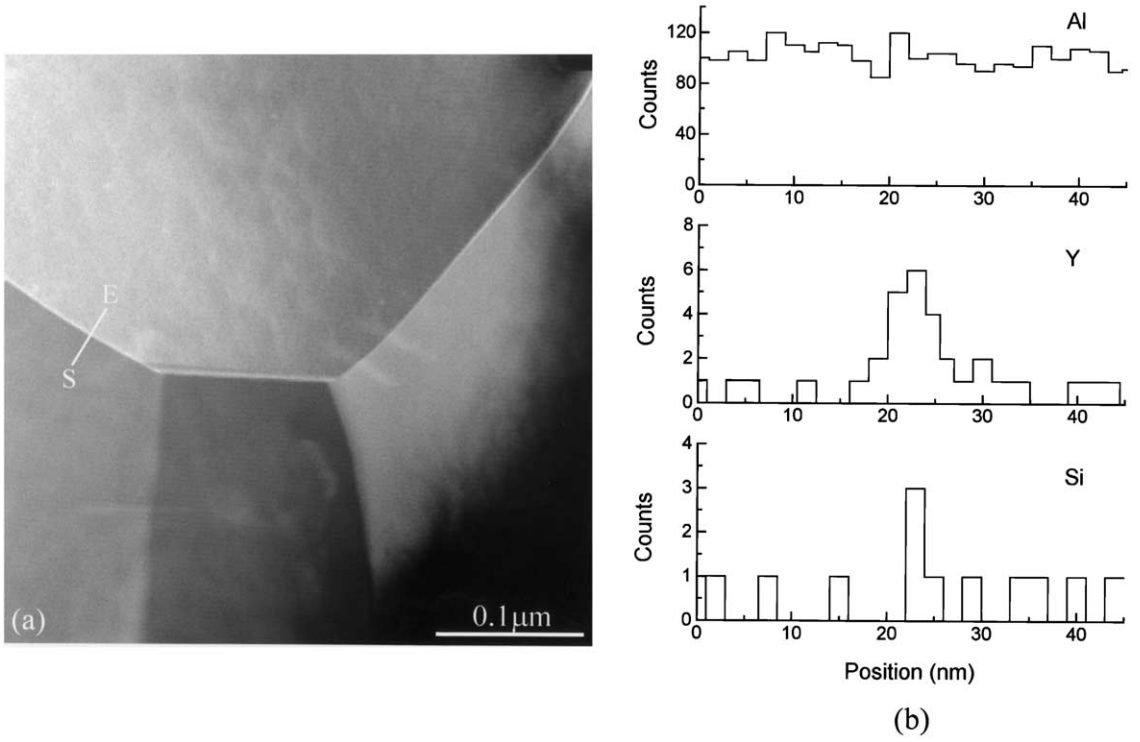

Fig. 5. (a) TEM micrograph showing the position of EDS line scanning across a grain boundary between two Al_2O_3 grains in Y^{3+} doped Al_2O_3–SiC composite and (b) detected signals along the scanning line for different elements.

3.3. Boundary chemistry

Fig. 4 shows a typical grain boundary between two Al_2O_3 grains in Y^{3+} doped Al_2O_3–SiC composite, indicating no amorphous phase at the Al_2O_3 grain boundary. In fact, all of the Al_2O_3 grain boundaries in the present Al_2O_3–SiC composites were clean in accordance to HRTEM observations. Therefore, the most possible boundary state is that rare-earth dopants segregated to the Al_2O_3 grain boundaries rather than formed the amorphous phase with Si^{4+} ions dissolved from SiC particles.

Chemical compositions on the Al_2O_3 grain boundaries were analyzed via an X-ray energy dispersive spectrometer (EDS) attached to the field emission type analytical TEM. A composition analysis by EDS line scanning on an Al_2O_3 grain boundary in Y^{3+} doped Al_2O_3–SiC composite with a probe diameter of 0.7 nm showed weak signals of Y and Si elements (Fig. 5). The weak element signals originate from the following facts: (1) native SiO_2 on SiC particle surfaces was removed during washing by the HF aqueous solution so that the amount of Si^{4+} ions diffusing into Al_2O_3 grain boundaries is very low; and (2) some of the Y^{3+} dopants were consumed to form Y-rich islands, as shown in Fig. 6. This implies that a rare-earth dopant level lower than 800 ppm could produce the fracture-mode change. Similar phenomena were observed in other Nd^{3+} and La^{3+} doped Al_2O_3–SiC composites.

It was understood that doping of rare-earth impurities in pure Al_2O_3 ceramics strengthened the Al_2O_3 boundary bonding.[4–7,13] The strong Al_2O_3 grain bonding in Al_2O_3–SiC composites should produce the transgranular fracture.[22–24] Logically, it can be deduced that the fracture-mode change in rare-earth doped Al_2O_3–SiC

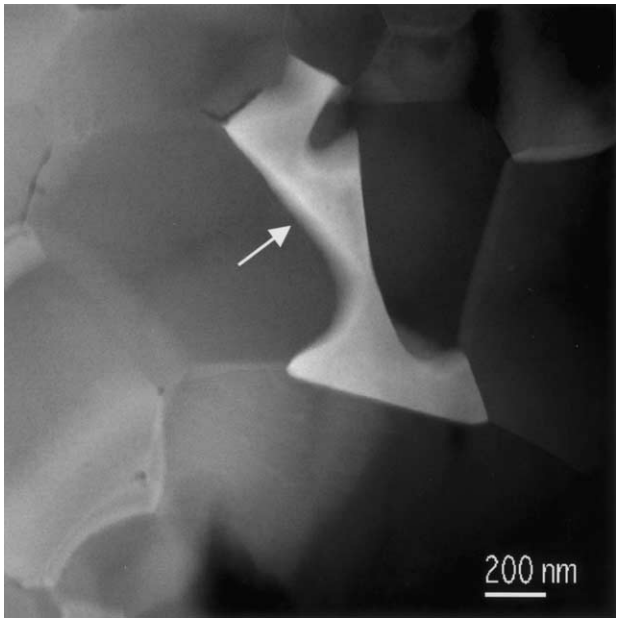

Fig. 6. TEM micrograph of Y^{3+} doped Al_2O_3–SiC composite, showing a Y-rich island (arrow) which consists of Y, Al and Si elements.

composites originated from a weak Al_2O_3 interface caused by the coaction of the rare-earth dopants and Si^{4+} ions dissolved from the SiC particle surfaces. In fact, some similar phenomena, that the coexistence of rare-earth oxides and other oxides weakens the interface bonding, has been found in $Al_2O_3/LaAl_{11}O_{18}$ composites[26–28] and SiC ceramics.[29]

4. Conclusions

The effects of doping of trace rare-earth impurities (Y^{3+}, Nd^{3+} and La^{3+}) on the microstructure and mechanical properties of Al_2O_3–5 vol.% SiC particle composites were investigated. The fracture toughness of rare-earth doped composites was higher than that of the dopant-free composites, due to a fracture-mode change and its resultant increased crack deflection. The intergranular fracture in rare-earth doped composites is believed to originate from a weak grain boundary bonding caused by segregation of rare-earth dopants and Si^{4+} ions dissolved from the SiC particle surfaces.

Acknowledgements

The authors are grateful to Drs. Yoshihisa Beppu and Guo-Jun Zhang for experimental assistance, and Dr. D. Doni Jayaseelan for invaluable discussion.

References

1. Bae, S. I. and Baik, S., Critical concentration of MgO for the prevention of abnormal grain growth in alumina. *J. Am. Ceram. Soc.*, 1994, **77**, 2499–2504.
2. Gavrilov, K. L., Bennison, S. J., Mikeska, K. R., Chabala, J. M. and Levi-Setti, R., Silica and magnesia dopant distributions in alumina by high-resolution scanning secondary ion mass spectrometry. *J. Am. Ceram. Soc.*, 1999, **82**, 1001–1008.
3. Park, C. W. and Yoon, D. Y., Effects of SiO_2, CaO_2, and MgO additions on the grain growth of alumina. *J. Am. Ceram. Soc.*, 2000, **83**, 2605–2609.
4. Cho, J., Harmer, M. P., Chan, H. M., Rickman, J. M. and Thompson, A. M., Effect of yttrium and lanthanum on the tensile creep behavior of aluminum oxide. *J. Am. Ceram. Soc.*, 1997, **80**, 1013–1017.
5. Wakai, F., Nagano, T. and Iga, T., Hardening in creep of alumina by zirconium segregation at the grain boundary. *J. Am. Ceram. Soc.*, 1997, **80**, 2361–2366.
6. Yoshida, H., Ikuhara, Y. and Sakuma, T., High-temperature creep resistance in rare-earth-doped, fine-grained Al_2O_3. *J. Mater. Res.*, 1998, **13**, 2597–2601.
7. Li, Y. Z., Wang, C. M., Chan, H. M., Rickman, J. M., Harmer, M. P., Chabala, J. M., Gavrilov, K. L. and Levi-Setti, R., Codoping of alumina to enhance creep resistance. *J. Am. Ceram. Soc.*, 1999, **82**, 1497–1504.
8. Le Gall, M., Huntz, A. M., Lesage, B., Monty, C. and Bernardini, J., Self-diffusion in α-Al_2O_3 and growth rate of alumina scales formed by oxidation: effect of Y_2O_3 doping. *J. Mater. Sci.*, 1995, **30**, 201–211.
9. Cho, J., Chan, H. M., Harmer, M. P. and Rickman, J. M., Influence of yttrium doping on grain misorientaion in aluminum oxide. *J. Am. Ceram. Soc.*, 1998, **81**, 3001–3004.
10. Gulgun, M. A., Putlayev, V. and Ruhle, M., Effects of yttrium doping α-alumina: I, microstructure and microchemistry. *J. Am. Ceram. Soc.*, 1999, **82**, 1849–1856.
11. Wang, C. M., Cargill, G. S. III, Harmer, M. P., Chan, H. M. and Cho, J., Atomic structural environment of grain boundary segregated Y and Zr in creep resistant alumina from EXAFS. *Acta Mater.*, 1999, **47**, 3411–3422.
12. Cho, J., Wang, C. M., Chan, H. M., Rickman, J. M. and Harmer, M. P., Role of segregating dopants on the improved creep resistance of aluminum oxide. *Acta Mater.*, 1999, **47**, 4197–4207.
13. Takigawa, Y., Ikuhara, Y. and Sakuma, T., Grain boundary bonding state and fracture energy in small amount of oxide-doped fine-grained Al_2O_3. *J. Mater. Sci.*, 1999, **34**, 1991–1997.
14. Niihara, K., New design concept of structural ceramics—ceramic nanocomposites. *J. Ceram. Soc. Jpn.*, 1991, **99**, 974–992.
15. Ohji, T., Hirano, T., Nakahira, A. and Niihara, K., Particle/matrix interface and its role in creep inhibition in alumina/silicon carbide nanocomposites. *J. Am. Ceram. Soc.*, 1996, **79**, 33–45.
16. Thompson, A. M., Chan, H. M. and Harmer, M. P., Tensile creep of alumina-silicon carbide "nanocomposites". *J. Am. Ceram. Soc.*, 1997, **80**, 2221–2228.
17. Deng, Z. Y., Zhang, Y. F., Shi, J. L. and Guo, J. K., Microstructure and flexure creep behaviour of SiC-particle reinforced Al_2O_3 matrix composites. *J. Eur. Ceram. Soc.*, 1996, **16**, 1337–1343.
18. Deng, Z. Y., Shi, J. L., Zhang, Y. F., Lai, T. R. and Guo, J. K., Creep and creep-recovery behavior in silicon-carbide-particle-reinforced alumina. *J. Am. Ceram. Soc.*, 1999, **82**, 944–952.
19. Jeong, Y. K., Nakahira, A. and Niihara, K., Effects of additives on microstructure properties of alumina-silicon carbide nanocomposites. *J. Am. Ceram. Soc.*, 1999, **82**, 3609–3612.
20. Fang, J. X., Thompson, A. M., Harmer, M. P. and Chan, H. M., Effect of yttrium and lanthanum on the final-stage sintering behavior of ultrahigh-purity alumina. *J. Am. Ceram. Soc.*, 1997, **80**, 2005–2012.
21. Thompson, A. M., Soni, K. K., Chan, H. M., Harmer, M. P., Williams, D. B., Chabala, J. M. and Levi-Setti, R., Dopant distributions in rare-earth-doped alumina. *J. Am. Ceram. Soc.*, 1997, **80**, 373–376.
22. Zhao, J., Stearns, L. C., Harmer, M. P., Chan, H. M., Miller, G. A. and Cook, R. F., Mechanical behavior of alumina-silicon carbide "nanocomposites". *J. Am. Ceram. Soc.*, 1993, **76**, 503–510.
23. Deng, Z. Y., Shi, J. L., Zhang, Y. F., Jiang, D. Y. and Guo, J. K., Pinning effect of SiC particles on mechanical properties of Al_2O_3-SiC ceramic matrix composites. *J. Eur. Ceram. Soc.*, 1998, **18**, 501–508.
24. Ohji, T., Jeong, Y. K., Choa, Y. H. and Niihara, K., Strengthening and toughening mechanisms of ceramic nanocomposites. *J. Am. Ceram. Soc.*, 1998, **81**, 1453–1460.
25. Faber, K. T. and Evans, A. G., Crack deflection processes. 1. theory. *Acta Metall.*, 1983, **31**, 565–576.
26. Yasuoka, M., Hirao, K., Brito, M. E. and Kanzaki, S., High-strength and high-toughness ceramics in the $Al_2O_3/LaAl_{11}O_{18}$ systems. *J. Am. Ceram. Soc.*, 1995, **78**, 1853–1856.
27. Brito, M. E., Yasuoka, M. and Kanzaki, S., In process surface modification of alumina grains in sintered bodies. *Ceram. Tans.*, 1996, **79**, 231–237.
28. Yasuoka, M., Hirao, K., Brito, M. E. and Kanzaki, S., Microstructure and mechanical properties of alumina based ceramics with changed amounts of β-lanthanaluminate. *J. Ceram. Soc. Japan*, 1997, **105**, 641–644.
29. Zhou, Y., Hirao, K., Toriyama, M., Yamauchi, Y. and Kanzaki, S., Effects of intergranular phase chemistry on the microstructure and mechanical properties of silicon carbide ceramics densified with rare-earth oxide and alumina additions. *J. Am. Ceram. Soc.*, 2001, **84**, 1642–1644.